ISSN 1027-5495. Functional Materials, 30, No.3 (2023), p. 332-337.
doi:https://doi.org/10.15407/fm30.03.332

Refractive index and optical dielectric function of $CdTe_{0.9}Se_{0.1}$ thin film produced by quasi-closed sublimation

A. Kashuba[1], *H. Ilchuk*[1], *I. Semkiv*[1], *I. Kuno*[2], *N. Pokladok*[1], *N. Ukrainets*[1]

[1]Department of General Physics, Lviv Polytechnic National University, 12 S. Bandera Str., 79013 Lviv, Ukraine
[2]Department of Optoelectronics and Information Technologies, Ivan Franko National University of Lviv, 107 Tarnavskyi Str., 79017 Lviv, Ukraine

Received May 29, 2023

Optical constants, dispersion and oscillator parameters of $CdTe_{0.9}Se_{0.1}$ thin film deposited onto quartz substrates by the quasi close-space sublimation method is studied. The study of optical functions is performed on the basis of the experimentally measured transmission spectrum by the Swanepoel method. The spectral behavior of optical functions, such as refractive index and dielectric functions is established. The refractive index was extrapolated by the Cauchy and Sellmeier dispersion relationships over the spectral range from 900 to 2500 nm. The dispersion of the refractive index is discussed in terms of the Wemple and Di Domenico single oscillator model. The spectral behavior of optical dielectric functions was studied in the framework of the Drude free electron model. For a thin $CdTe_{0.9}Se_{0.1}$ film, the optical mobility, optical resistance, relaxation time, plasma frequency, and carrier concentration are determined for the first time.

Keywords: thin films, refractive index, optical dielectric function, relaxation time, optical mobility.

Показник заломлення і оптичні діелектричні функції тонкої плівки $CdTe_{0.9}Se_{0.1}$ осадженої методом квазізамкненого об'єму. *А. Кашуба, Г, Ільчук, І. Семків, І, Куньо, Н, Покладок, Н, Українець*

Оптичні константи, дисперсія та параметри осцилятора досліджено для тонкої плівки $CdTe_{0.9}Se_{0.1}$ осадженої на кварцову підкладку за допомогою методу квазізамкнутого об'єму. Дослідження оптичних функцій виконано на основі експериментально виміряного спектру пропускання методом Свейнпола. Встановлено спектральну поведінку оптичних функцій, таких як показник заломлення та діелектрична функція. Показник заломлення екстраполювали за допомогою дисперсійних співвідношень Коші та Зелмайєра в спектральному діапазоні від 900 до 2500 нм. Дисперсія показника заломлення обговорюється в межах одноосциляторної моделі Вемпла і Ді Доменіко. Спектральну поведінку оптичних діелектричних функцій досліджено в рамках моделі вільних електронів Друде. Для тонкої плівки $CdTe_{0.9}Se_{0.1}$ вперше встановлено оптичну рухливість, питомий оптичний опір, час релаксації, плазмову частоту та концентрацію носіїв.

1. Introduction

CdTe semiconductor has proven to be a leading compound for manufacturing cost-effective second-generation photovoltaic devices. CdTe-based solar cells attract much attention from researchers since CdTe is characterized by a directly forbidden gap with an energy bandwidth of ~ 1.4 eV [1]

and a high absorbance (above 10^5 cm^{-1}) [1]. This makes it an excellent light-absorbing layer for solar cells. When forming high-efficiency heterojunctions based on *p*-CdTe used as window layers of solar batteries, cadmium sulfide is mainly employed [2]. CdS is characterized by a high absorbance and high photoconductivity in the visible region. In the solar cells based on the CdS/CdTe heterojunctions, the thickness of the CdS layer in most cases is about 150–300 nm [3]. In this case, photogenerated charge carriers almost completely recombine inside the CdS film and do not generate photocurrent.

The occurrence of photocurrent is also negatively affected by the lattice mismatch between CdTe and CdS layers. Despite the reduction in the lattice mismatch between the CdTe and CdS layers due to the formation of CdS_xTe_{1-x} ($CdTe_xS_{1-x}$) solid solutions, a high defect density causes a loss of efficiency [4]. CdSe can be an alternative solution to the problems originating from CdTe/CdS junction. In recent years $CdTe_{1-x}Se_x$ solid solution is one of the promising materials to improve solar cells [5]. $CdTe_{1-x}Se_x$ thin films with the desired composition can be easily synthesized by numerous methods (high-vacuum evaporation of the certain elements [6] or solid solution based on them [7]; co-evaporation of CdTe and CdSe [8]; close space sublimation [9]; hot wall deposition [10]; molecular beam epitaxy [11]; electron beam deposition [12]; electrodeposition [13]). $CdTe_{1-x}Se_x$ forms cubic (zinc blende) and hexagonal (wurtzite) phases, depending mainly on the choice of method for its synthesis and on the specific growth parameters [9, 13, 14, 15]. But for solar cells, only the cubic structure of $CdTe_{1-x}Se_x$ is acceptable due to its photoactivity and ability to convert light into photocurrent, while the hexagonal structure is not photoactive [14].

The aim of the present work is the investigation of the optical properties of $CdTe_{1-x}Se_x$ thin films produced on quartz substrate by the quasi close-space sublimation (quasi-CSS) method. The transmittance spectra in the visible and near-infrared regions (900–2500 nm) are studied at room temperature. Refractive index and optical dielectric function are determined from the measurements of transmittance spectra.

2. Experimental

$CdTe_{1-x}Se_x$ thin films were deposited on quartz substrates using the quasi-CSS technique at a pressure of $1 \cdot 10^{-6}$ Torr [16, 17]. Polycrystalline $CdTe_{0.5}Se_{0.5}$ powder was used as the source. The temperatures of the source and the substrate were 900 K and 700 K, respectively. The temperature was controlled using a PID regulator of temperature PE-202, using a thermocouple of the "K" type. The relative error in temperature did not exceed 0.2 %. The substrates 14 mm in diameter were used for deposition of $CdTe_{1-x}Se_x$ thin films. Before the film deposition, the substrate surface was cleaned by boiling in a high-purity CCl_4 solution during 0.5 h.

As a result, $CdTe_{1-x}Se_x$ thin films with a thickness of ~ 1.2 μm were obtained (as estimated from measurements with a Veeco profilometer). According to X-ray diffraction (XRD) analysis, the $CdTe_{1-x}Se_x$ thin film is a single-phase and crystallizes in a cubic structure (unit-cell dimensions a = 0.6395(3) nm and V = 0.2616(4) nm^3 [17]). The energy dispersive X-ray (EDX) analysis was used to estimate the chemical and component composition of the thin film. Based on XRD and EDX, the content of Se was x = 0.1 in the sample. The Se content in this polycrystalline film is much lower than that in the source (i.e., in the polycrystalline $CdTe_{0.5}Se_{0.5}$ powder). The same situation was described in [18]. It is also observed when the $Cd_{1-x}Zn_xTe$ and $Cd_{1-x}Mn_xTe$ films are deposited. This phenomenon is due to nonequilibrium deposition in the CSS-growing process [18, 19]. The results of the XRD and EDX analysis were reported early in [17].

The optical transmission spectra (Shimadzu UV-3600) of the obtained samples were studied in the visible and near infrared regions at room temperature. Spectra of the optical transmission, reflection and absorbance in visible and near-infrared regions (400–2500 nm) were discussed in [16]. Also in [16], absorption and extinction coefficients were estimated from the spectra of the optical transmission and reflection.

In this work, the refractive index and optical dielectric functions were estimated for $CdTe_{0.9}Se_{0.1}$ thin film by the Swanepoel method [20, 21]. This method is applicable in the case of a weakly absorbing thin film on an entirely transparent substrate that is much thicker than the thin film. These conditions are met in this work.

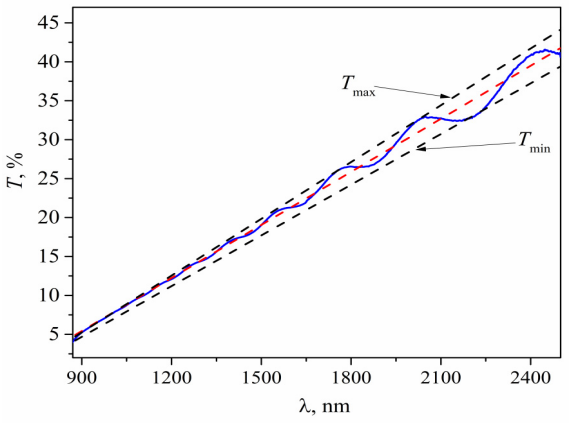

Fig. 1. Blue line — the experimentally obtained transmission spectra of $CdTe_{0.9}Se_{0.1}$ thin film and substrate in the transparency region; dashed line — envelope curves for interference maxima — T_{max} and minima — T_{min}; green line — linear fitting of experimental transmission spectra.

The refractive index $n(\lambda)$ of the $CdTe_{0.9}Se_{0.1}$ thin film can be calculated using the following equation:

$$n = \sqrt{N + (N^2 - n_s^2)^{1/2}}, \quad (1)$$

$$N = 2 \cdot n_s \cdot \frac{T_{max} - T_{min}}{T_{max} \cdot T_{min}} + \frac{2 \cdot n_s^2 + 1}{2},$$

where n_s is the refractive index of the substrate:

$$n_s = \frac{1}{T_s} + \sqrt{\frac{1}{T_s^2} - 1}, \quad (2)$$

T_s is the transmittance of the substrate in the transparent zone. Spectral behavior of the T_s for quartz substrate is described in [22]. It should be emphasized that Eq. (1) is valid only within the interference zone. Outside this zone, the refractive index can be determined using an extrapolation of calculated data [23].

The real and imaginary parts, ε_1 and ε_2, of the complex dielectric permittivity ε,

$$\varepsilon = \varepsilon_1 + i\varepsilon_2, \quad (3)$$

are related to the refractive index n and extinction coefficient k by Eqs. (4) and (5),

$$\varepsilon_1 = n^2 - k^2, \quad (4)$$

$$\varepsilon_2 = 2nk. \quad (5)$$

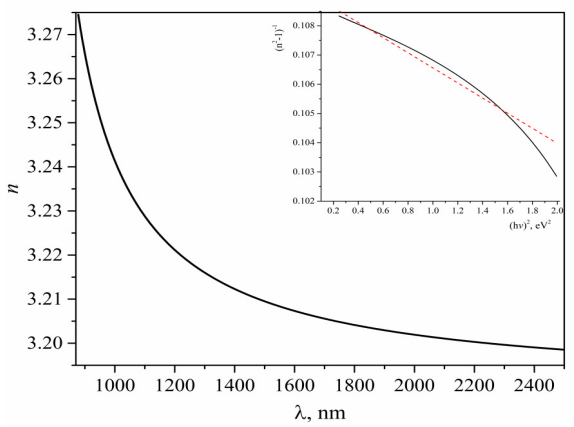

Fig. 2. Refractive index $n(\lambda)$ as a function of wavelength for $CdTe_{0.9}Se_{0.1}$ thin film. Inset — refractive index in coordinates $(n^2 - 1)^{-1} = f(h\nu)^2$, red line — linear fitting.

3. Results and discussion

Fig. 1 shows the combination of the transmission spectra of the $CdTe_{0.9}Se_{0.1}$ thin film and substrate in the transparency region (900–2500 nm). The total transmission spectrum of the $CdTe_{0.9}Se_{0.1}$ thin film and substrate in the range between 400 and 2500 nm was given in [16]. The transmission coefficient strongly depends on the film structure, which is determined by the preparation methods, film thickness and deposition conditions. The transmission spectra of the thin films exhibit periodic peaks and minima associated with interference effects, indicating the high structural perfection of thin films. A very rough surface will destroy the interference due to multiple reflections. The envelop curves of T_{max} and T_{min} can be obtained by extrapolation of experimentally determined points of location of interference maxima and minima (Fig. 1).

The dependence of the refractive index on wavelength is shown in Fig. 2. The refractive index of the thin film decreases with increasing wavelength. The dispersion spectrum of the refractive index was fitted using the Cauchy formula [24]:

$$n = A + \frac{B}{\lambda^2} + \frac{C}{\lambda^4}, \quad (6)$$

where A, B and C are the Cauchy's parameters. For $\lambda \to \infty$, the significance of the A parameters appears immediately as n_∞. Also, we note that for the analysis of the refractive index by Eq. (6) we used two representations of the Cauchy formula, with and without the inclusion of the parameter C.

Table I. Cauchy and Sellmeier parameters obtained from approximation of the spectral dependence of the refractive index for $CdTe_{0.9}Se_{0.1}$ thin film

Model		Parameters			n_∞	R^2
Cauchy	$\sim\lambda^{-4}$	A = 3.1993	B = −24488.5996	C = 6.82626·10^7	3.1993	0.996
	$\sim\lambda^{-2}$	A = 3.18731	B = 54361.52729	–	3.18731	0.965
Sellmeier		α = 2.18761	β = 24169.63439		3.18761	0.967

Table II. Wemple and Di Domenico parameters obtained from approximation of the spectral dependence of the refractive index for $CdTe_{0.9}Se_{0.1}$ thin film

E_0, eB	E_d, eB	n_0	M_{-1}	M_{-3}, eB^{-2}	f, eB^2	β, eB
6.50	59.59	3.19	9.17	0.28	387.335	0.93

Another model used in studying the dispersion of the refractive index is the Sellmeier model [25], which gives:

$$n = 1 + \frac{\alpha\lambda^2}{\lambda^2 - \beta}, \quad (7)$$

where α and β are the Sellmeier parameters. Under these conditions we can see that $n_\infty \approx (1 + \alpha)$, and the calculated values are given in Table I.

The dispersion of the refractive index is normal ($\Delta n/\Delta\lambda < 0$) and it is well described by the single oscillator model. In the inset of Fig. 2, the lines show the fitting of experimental points using the single oscillator model in the form proposed by Wemple and Di Domenico [26]:

$$n(h\nu)^2 - 1 \cong \frac{E_d \cdot E_0}{E_0^2 - (h\nu)^2} \quad (8)$$

were E_0 is the single oscillator energy; E_d is the dispersion energy; and $h\nu$ is the photon energy. Both Wemple parameters can be obtained from the slope and y-intercept of the plot, $(n^2 - 1)^{-1} = f(h\nu)^2$. The values of these parameters are summarized in Table II.

The refractive index $n_0 = n$ ($h\nu = 0$ eV) can be determined by Eq. (9).

$$n_0 = \sqrt{1 + \frac{E_d}{E_0}}. \quad (9)$$

The M_{-1} and M_{-3} moments of the optical spectra can be obtained from the following relations [27]:

$$E_0^2 = \frac{M_{-1}}{M_{-3}}, \quad E_d^2 = \frac{M_{-1}^3}{M_{-3}}. \quad (10)$$

The oscillator strength (f) is expressed according to Wemple and Di Domenico via the following formula [28]:

$$f = E_0 E_d. \quad (11)$$

Also, E_d is the measure of the strength of interband optical transitions that obeys the simple empirical relationship:

$$E_d = \beta N_c Z_a N_e, \quad (12)$$

N_c is the coordination number of the cation closest to the anion, Z_a is the formal chemical valency of the anion, N_e is the effective number of valence electrons per anion. In our cause, $N_c = 4$, $Z_a = 2$ and $N_e = 8$. Using Eq. (12) we obtained the value $\beta \approx 0.93$ eV. β essentially takes on two values: the "ionic" value $\beta_i = 0.26 + 0.04$ eV for halides and most oxides, and the "covalent" value $\beta_c = 0.37 + 0.05$ eV for $A^N B^{8-N}$ type structures [29]. We can assume that this behavior is associated with a decrease in the dispersion of energy levels [30] upon going from 3D crystal to 2D thin film.

The calculated spectral distributions of the optical dielectric function are shown in Fig. 3 and 4. For the values of n much greater than k, the value of ε_1 is approximately equal to n^2, and the dependence of $\varepsilon(\lambda)$ can be fitted using the relation [31] valid for the free electron light absorption,

$$\varepsilon_1 = n^2 = \varepsilon_\infty - \left(\frac{e^2}{\pi \cdot c^2}\right) \cdot \left(\frac{N_c}{m^*}\right) \cdot \lambda^2, \quad (13)$$

where c is the speed of light, m^* is the effective mass of the carrier, N_c is the carrier density, e is the electron charge, and ε_∞ is the high-frequency dielectric constant.

Table III. Energy properties of the $CdTe_{0.9}Se_{0.1}$ thin film

ε_∞	(N_c/m^*), kg^{-1} m^{-3}	N_c, m^{-3}	ω_p, s^{-1}	τ, s	μ_{opt}, m^2/V·s	ρ_{opt}, $\Omega^{-1}\cdot m^{-1}$
10.31	$1.62\cdot10^{47}$	$4.8\cdot10^{93}$	$2.16\cdot10^{10}$	$8.76\cdot10^{3}$	$4.75\cdot10^{-62}$	$3.63\cdot10^{-11}$

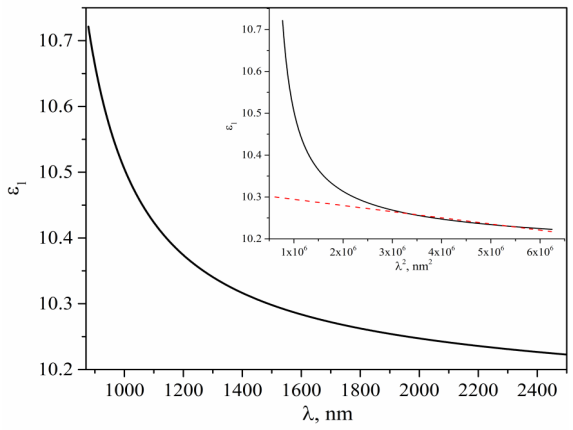

Fig. 3. Real part of the optical dielectric function $\varepsilon_1(\lambda)$ as a function of wavelength for $CdTe_{0.9}Se_{0.1}$ thin film. Inset — real part of the optical dielectric function in coordinates $\varepsilon_1 = f(\lambda^2)$, red line — linear fitting.

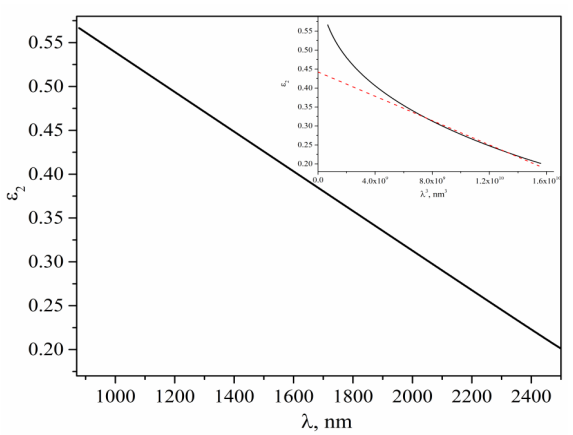

Fig. 4. Imaginary part of the optical dielectric function $\varepsilon_2(\lambda)$ as a function of wavelength for $CdTe_{0.9}Se_{0.1}$ thin film. Inset — imaginary part of the optical dielectric function in coordinates $\varepsilon_2 = f(\lambda^3)$, red line — linear fitting.

To obtain the high frequency dielectric constant ε_∞, we plot a graph n^2 as a function of λ^2 and extrapolate the linear part of the curve to $\lambda^2 = 0$ (Fig. 3, inset).

Furthermore, the dispersion of the imaginary part of the dielectric function $\varepsilon_2(\lambda)$ is used to estimate the relaxation time (τ), optical mobility (μ_{opt}) and optical resistivity (ρ_{opt}) in the Drude free electron model [31, 32] using the relation,

$$\varepsilon_2 = \left(\frac{e^2}{4\varepsilon_0\pi^3 \cdot c^3}\right)\cdot\left(\frac{N_c}{m^*}\right)\cdot\left(\frac{1}{\tau}\right)\lambda^3. \qquad (14)$$

The parameter τ is found from the slope of the plot $\varepsilon_2(\lambda)^3$, where the value of N_c/m^* is taken from Eq. (13). Afterwards, the optical mobility μ_{opt} and optical resistivity ρ_{opt} of the $CdTe_{0.9}Se_{0.1}$ thin film are calculated by the relations (15) and (16) [31, 32],

$$\mu_{opt} = \frac{e\tau}{m^*}, \qquad (15)$$

$$\rho_{opt} = \frac{1}{e\mu_{opt}N_c}. \qquad (16)$$

The calculated values of the relaxation time τ, optical mobility μ_{opt} and optical resistivity ρ_{opt} are given in Table III.

Additionally, the electron plasma frequency (ω_p) is calculated using the relation [31]:

$$\omega_p = \left(\frac{e^2N_c}{\varepsilon_0 m^*}\right)^{1/2}. \qquad (17)$$

Carrier concentration of the $CdTe_{0.9}Se_{0.1}$ thin film can be calculated using the well-known relation of the semiconductor theory:

$$N_c = 2\left(\frac{2\pi m^* kT}{h^2}\right)^{3/2}, \qquad (18)$$

where T is thermodynamic temperature. In our case, measurement was made at room temperature (T ~ 293 K). The effective mass of the carrier m^* was taken from Eq. (13). As result, we obtained the value of carrier concentration near $4.8\cdot10^{93}$ m^{-3} in the $CdTe_{0.9}Se_{0.1}$ thin film at room temperature.

4. Conclusions

The refractive index and optical dielectric functions of the $CdTe_{0.9}Se_{0.1}$ thin film are determined as functions of the wavelength using the Swanepoel method. The dispersion of the refractive index is normal

and was successfully fitted with the Cauchy and Sellmeier dispersion relationships, and good agreement between the models is observed. Also, the dispersion of the refractive index was studied in the framework of the Wemple and Di Domenico single oscillator model. Based on this model, single oscillator energy, dispersion energy, oscillator strength and moments (M_{-1} and M_{-3}) of the optical spectra were obtained. It has been established that the "covalent" value of β for polycrystalline thin films is higher than for single crystals. The optical mobility, optical resistivity, relaxation time, plasma frequency and carrier concentration were obtained from the spectral distribution of optical dielectric functions in the framework of the Drude free electron model. These parameters (optical mobility, optical resistivity, relaxation time and carrier concentration) for the studied $CdTe_{1-x}Se_x$ ($x = 0.1$) thin film have been estimated for the first time.

Acknowledgment. This research was funded by the Ministry of Education and Science of Ukraine, Project of Young Scientists number 0121U108649.

References

1. N.Romeo, A.Bosio, R.Tedeschi et al., *Mater. Chem. Phys.*, **66**, 201 (2000).
2. N.Romeo, A.Bosio, V.Canevari et al., *Sol. Energy.*, **77**, 795 (2014).
3. A.Bosio, N.Romeo, S.Mazzamuto et al., *Growth Charact. Mater.*, **52**, 247 (2006).
4. B.B.Dumre, N.J.Szymanski, V.Adhikari et al., *Sol. Energy*, **194**, 742 (2019).
5. T.Ablekim, J.N.Duenow, X.Zheng et al., *ACS Energy Lett.*, **5**, 892 (2020).
6. M.A.Russak, C.Creter, *J. Electrochem. Soc.*, **131**, 556 (1984).
7. M.El-Nahass, M.M.Sallam, M.A.Afifi et al., *Mater. Res. Bull.*, **42**, 371 (2007).
8. M.Lingg, A.Spescha, S.G.Haass et al., *Sci. Technol. Adv. Mater.*, **19**, 683 (2018).
9. D.E.Swanson, J.R.Sites, W.S.Sampath, *Sol. Energy Mater. Sol. Cells*, **159**, 389 (2017).
10. N.Muthukumarasamy, R.Balasundaraprabhu, S.Jayakumar et al., *Phys. Stat. Sol. (A)*, **201**, 2312 (2004).
11. F.Amir, K.Clark, E.Maldonado et al., *J. Cryst. Growth*, **310**, 1081 (2008).
12. R.Islam, H.Banerjee, D.Rao, *Thin Solid Films*, **266**, 215 (1995).
13. M.Bouroushian, Z.Loizos, N.Spyrellis et al., *Thin Solid Films*, **229**, 101 (1993).
14. J.D.Poplawsky, W.Guo, N.Paudel et al., *Nat. Commun.*, **7**, 12537 (2016).
15. L.Kumar, B.P.Singh, A.Misra et al., *Phys. B Condens. Matter.*, **363**, 102 (2005).
16. R.Petrus, H.Ilchuk, A.Kashuba et al., *Molecular Crystals and Liquid Crystals*, **717**, 128 (2021).
17. A.I.Kashuba, H.A.Ilchuk, R.Y.Petrus et al., *Applied Nanoscience (Switzerland)*, **12**, 335 (2022).
18. H.Ilchuk, E.Zmiiovska, R.Petrus et al., *J. Nano- and Electron. Phys.*, **12**, 01027 (2020).
19. V.Kosyak, A.Opanasyuk, P.M.Bukivskij et al., *J. Cryst. Growth.*, **312**, 1726 (2010).
20. Y.Jin, B.Song, Z.Jia et al., *Optics Express*, **25**, 440 (2017).
21. R.Petrus, H.Ilchuk, A.Kashuba et al., *Functional Materials*, **27**, 342 (2020).
22. H.A.Ilchuk, A.I.Kashuba, R.Y.Petrus et al., *Physics and Chemistry of Solid State*, **21**, 57 (2020).
23. J.S.Gonzalez, A.D.Parralejo, A.L.Ortiz et al., *Appl. Surf. Sci.*, **252**, 6013 (2006).
24. M.Born, E.Wolf, Principles of Optics. Ch. II. Pergamon Press, Oxford (1975).
25. A.Ashour, N.El-Kadry, S.A.Mahmoud, *Thin Solid Films*, **269, 117 (1995).**
26. S.H.Wemple, M.DiDomenico, *Phys. Rev. B.*, **3**, 1338 (1971).
27. Y.Caglar, S.Ilican, M.Caglar, *Eur. Phys. J. B*, **58**, 251 (2007).
28. A.Kocyigit, M.O.Erdal, M.Yildirim, *Zeitschrift fur Naturforschung*, **74**, 1 (2019).
29. R.Swanepoel, *J. Phys. E, Sci. Instrum.*, **16**, 1214 (1983).
30. H.A.Ilchuk, B.Andriyevsky, O.S.Kushnir et al., *Ukr. J. Phys. Opt.*, **22**, 101 (2021).
31. A.Y.Fasasi, E.Osagie, D.Pelemo et al., *Am. J. Mater. Synth. Process.*, **3**, 12 (2018).
32. A.M.Alsaad, A.A.Ahmad, Q.M.Al-Bataineh et al., *Materials*, **13**, 1737 (2020). — refractive index in coordinates $(n^2 - 1)^{-1} = f(h\nu)^2$, red line — linear fitting. imaginary part of the optical dielectric function in coordinates $\varepsilon_2 = f(\lambda^3)$, red line — linear fitting.